9022 *Biochemistry* **2009,** *48,* 9022–9030
DOI: 10.1021/bi901124j

BIOCHEMISTRY
including biophysical chemistry & molecular biology
*Article*

# Urea-Induced Unfolding of Na,K-ATPase As Evaluated by Electron Paramagnetic Resonance Spectroscopy†

Mohammad Babavali,‡ Mikael Esmann,‡ Natalya U. Fedosova,‡ and Derek Marsh*,§

‡*Department of Physiology and Biophysics, Aarhus University, Aarhus, Denmark, and* §*Max-Planck-Institut für biophysikalische Chemie, Abt. Spektroskopie, 37077 Göttingen, Germany*

*Received July 2, 2009; Revised Manuscript Received August 18, 2009*

ABSTRACT: Urea-induced unfolding of Na,K-ATPase from pig kidney and from shark salt gland was studied by electron paramagnetic resonance (EPR) spectroscopy of a nitroxyl derivative of maleimide covalently attached to sulfhydryl groups which are essential for activity. Urea-induced structural changes lead to the inhibition of Na,K-ATPase activity. Structural changes detected by EPR are reversible over the whole range of urea concentrations (0−8 M), although activity loss is always irreversible. The structure of the cytoplasmic domain is more accessible and more susceptible to perturbations than is the transmembrane sector of the Na,K-ATPase and thus is more sensitive to denaturant. Conformational changes at the active thiol groups of these enzymes indeed take place before unfolding of the enzyme as a whole, together with enzyme inactivation. Na,K-ATPase from pig kidney is more stable not only to thermal denaturation but also to urea-induced denaturation than is the Na,K-ATPase from shark salt gland. Susceptibility of the latter could arise from the nonhomologous regions in the cytoplasmic domain.

The sodium−potassium pump is a membrane-bound Na,K-ATPase enzyme that is responsible for maintaining ionic homeostasis in animal cells. The transmembrane section of the protein comprises 10 transmembrane helices from the α-subunit, together with the single transmembrane helices of the *β*- and *γ*-subunits (*1*, *2*). The α-subunit has a large cytoplasmic domain that contains the enzymatic active site.

The protein from shark salt gland or from pig kidney contains 23 cysteine residues situated at homologous positions in the α-subunit. These sulfhydryl groups of the Na,K-ATPase (*3*, *4*) are in part critical for enzymatic function (*5*−*11*) and also provide convenient sites for attachment of spectroscopic probes to the membranous enzyme. Reactivity toward *N*-ethylmaleimide (NEM)[1] has been used to classify the sulfhydryl-bearing residues of the enzyme from shark salt gland into those which do not affect activity (class I groups, approximately two per α-subunit) and those which are essential for activity (class II groups, approximately five groups per α-subunit) (*9*, *10*). Within the class II groups, modification of the single residue that is protected in the presence of ATP and $K^+$ abolishes activity entirely, whereas modification of the other class II groups yields an enzyme that is able to support only the partial reaction of phosphorylation from ATP (*6*, *7*, *12*). Only six to seven of the total of 23 −SH groups are labeled by NEM in the membranous enzyme from the salt gland of *Squalus acanthias* (*9*), and these are essentially confined to the α-subunit (*10*). For the enzymes from both pig kidney and shark salt gland, only six of the 23 cysteine residues are contained in the transmembrane section of the protein with the remainder residing in the cytoplasmic domain, which accounts for most of the mass of the protein (*1*, *2*). Only three of the nine cysteine residues that are labeled with NEM are found in the trypsinized fragment of Na,K-ATPase from shark salt gland (*13*, *14*).

Spin-labeled derivatives of maleimide, such as 5-MSL, have been used both to detect conformational changes within the enzyme (*9*) and to study the overall rotational diffusion of the protein by means of saturation transfer EPR spectroscopy (*15*, *16*). The EPR spectra of integral membrane proteins spin-labeled with 5-MSL, including Na,K-ATPase, are generally characterized by the coexistence of two spectral components with very different states of probe mobility. These components are commonly called strongly and weakly immobilized and are associated with restricted and less restricted motion on the 9.4-GHz EPR time scale for nitroxide motion. Protein unfolding is expected to increase the population of weakly immobilized residues, relative to the strongly immobilized spin-label population, and therefore, EPR can be used as a structural probe of protein unfolding and refolding.

In this work, we study the urea-induced unfolding of Na,K-ATPase from shark salt gland and from pig kidney by EPR spectroscopy of a nitroxyl derivative of maleimide (5-MSL) that is covalently attached to the class II sulfhydryl groups, which are essential for activity. There is a strong structural and sequence homology between the shark and mammalian enzymes (ca. 94% between shark and pig) (*1*, *2*). Nevertheless, the Na,K-ATPases from the two sources differ considerably in their thermal stability and denaturation temperatures (*17*). It is therefore of considerable interest to compare the sensitivities to unfolding by urea, as detected by probes attached to homologous residues. Here, we

†M.B. acknowledges support from the Marie Curie Early Stage Training in BIOMEM, Grant MEST-CT-2004-007931. M.E. acknowledges financial support from the Aarhus University Research Foundation (Grant E-2006-SUN-1-89).

*To whom correspondence should be addressed: Max-Planck-Institut für biophysikalische Chemie, Abt. Spektroskopie, 37070 Göttingen, Germany. Telephone: +49 551 201 1285. Fax: +49 551 201 1501. E-mail: dmarsh@gwdg.de.

[1]Abbreviations: 5-MSL, 3-maleimido-2,2,5,5-tetramethylpyrrolidine-*N*-oxyl; CDTA, *trans*-1,2-cyclohexylenedinitrilotetraacetic acid; EDTA, ethylenediaminetetraacetic acid; EPR, electron paramagnetic resonance; NEM, *N*-ethylmaleimide; K-pNPPase, $K^+$-*p*-nitrophenylphosphatase; SDS, sodium dodecyl sulfate.

 Published on Web 08/21/2009 

correlate the structural changes monitored using EPR with loss of activity by both enzymes and with rates of inactivation by modification with NEM, and we extract effective thermodynamic parameters for the unfolding of the two Na,K-ATPases. Whereas denaturant-induced unfolding of soluble proteins with urea or guanidine hydrochloride is extensively studied, this is currently not the case for large integral membrane transport systems (but see ref *18*), which provides further motivation for studies with the Na,K-ATPase.

## MATERIALS AND METHODS

*Enzyme Preparation*. Membranous Na,K-ATPase was prepared from the salt gland of *S. acanthias* according to the method of Skou and Esmann (*19*), but omitting the treatment with saponin. Na,K-ATPase from pig kidney microsomal membranes was prepared using pretreatment with SDS and purified by differential centrifugation (*20*, *21*). The Na,K-ATPase constituted typically 70% of the total protein (determined as the content of α- and β-subunits from SDS gel electrophoresis).

*Na,K-ATPase Activity Assays*. Steady-state Na,K-ATPase activity was assayed at 37 °C [130 mM NaCl, 20 mM KCl, 4 mM $MgCl_2$, 3 mM ATP (Tris salt), and 20 mM histidine (pH 7.4) in the assay medium] by measuring the liberation of phosphate from ATP with colorimetric methods (*22*, *23*). The specific activity of both enzyme preparations was approximately 30 μmol of ATP hydrolyzed (mg of protein)$^{-1}$ min$^{-1}$. Inactivation by urea was studied by incubating 0.5 mg/mL purified enzyme with 20 mM histidine, 150 mM KCl, and various concentrations of urea for 24 h at 0 °C. The enzyme activity was then assayed at 37 °C, as described above. The effect of urea on inactivation by NEM was studied by first incubating the enzyme in 150 mM KCl, 5 mM CDTA, and 20 mM histidine containing different concentrations of urea for 30 min at 22 °C. Then 2 mM NEM was added, and activity measurements were performed at 37 °C after incubation at 22 °C for different periods of time.

*Prelabeling of Na,K-ATPase Membranes with NEM*. Prelabeling of shark Na,K-ATPase with NEM to block class I −SH groups was performed as follows (*10*). Na,K-ATPase (~1 mg/mL) was incubated at 20 °C with 0.1 mM NEM in 30 mM histidine (pH 7.0 at 23 °C), 5 mM CDTA, 150 mM KCl, and 36% (v/v) glycerol for 60 min. The reaction was stopped by addition of 1 mM 2-mercaptoethanol, and the membranes were washed by centrifugation in 20 mM histidine (pH 7.0 at 20 °C) and 25% (v/v) glycerol at 200000*g*. Three centrifugations in 27 mL tubes were sufficient to remove residual reaction medium. The prelabeled shark enzyme was stored in 20 mM histidine and 25% (v/v) glycerol at −20 °C. Prelabeling of pig kidney Na,K-ATPase followed the same route, except that 10 mM NEM was used, and the reaction was stopped by addition of an equal volume of 20 mM histidine (pH 7.0 at 20 °C) and 10% (v/v) glycerol containing 12 mM 2-mercaptoethanol. The membranes were washed twice by centrifugation in 20 mM histidine, 250 mM sucrose, and 1 mM EDTA (pH 7.0) at 200000*g* and stored in this buffer. The NEM-prelabeled enzymes had more than 90% of the initial specific activity.

*Spin Labeling of Class II Sulfhydryl Groups*. The maleimide nitroxide spin-label derivative 5-MSL was obtained from Sigma-Aldrich, Inc. (St. Louis, MO). Selective spin labeling of the class II −SH groups, which are essential for the overall Na,K-ATPase activity, was performed as follows (*9*). Prelabeled shark Na,K-ATPase was incubated with 100 μM 5-MSL at 37 °C in 30 mM histidine (pH 7.4 at 37 °C) in the presence of 150 mM KCl, 5 mM CDTA, and 3 mM ATP (Tris salt). The reaction was stopped by addition of 1 mM 2-mercaptoethanol, and the membranes were washed by centrifugation at 200000*g* in 20 mM histidine (pH 7.0 at 20 °C) and 25% (v/v) glycerol. Under these conditions, more than 90% of the label resides in the α-subunit (ref *10*, with molecular masses of 8.8, 29, and 100 nmol/mg for α-, β-, and γ-subunits, respectively). The spin-labeled shark enzyme was stored in 20 mM histidine and 25% (v/v) glycerol at −20 °C. The residual activity was approximately 10% of that of the unlabeled enzyme. Pig kidney Na,K-ATPase was spin labeled in a similar fashion, except that 1.0 mM 5-MSL was used. The washing buffer contained 20 mM histidine, 250 mM sucrose, and 1 mM EDTA (pH 7.0), and the membranes were stored in this buffer. The residual activity of MSL-labeled pig kidney Na,K-ATPase was approximately 20% of that of the unlabeled enzyme.

*EPR Spectroscopy*. Samples for EPR spectroscopy were prepared according to the following protocol (*15*): 3 mg of Na,K-ATPase spin labeled with 5-MSL were incubated for 10 min at 22 °C with 9.7 mL of buffer containing 30 mM histidine (pH 7), 100 mM KCl, 5 mM CDTA, and varying concentrations of urea. Membranes were pelleted by centrifugation at 100000*g* at 10 °C for 45 min, and the pellet was then taken up into a 100 μL glass capillary and used for EPR measurements. Variable-temperature measurements were performed from 0 to 37 °C, over a period of hours. At the end of each temperature series, the spectrum was re-recorded at 0 °C to check that no time-dependent changes had taken place during the period of the experiment. A further control experiment indicated that no time-dependent changes occurred upon incubation of the sample for 14 h in 4 M urea at 0 °C. After each set of variable-temperature measurements, the sample was washed with 10 mL of buffer containing 30 mM histidine (pH 7), 100 mM KCl, and 5 mM CDTA to remove urea and pelleted by centrifugation at 100000*g* and 10 °C for 45 min. The pellet was then taken up again in a 100 μL glass capillary and used for further EPR measurement.

EPR measurements were carried out on a 9-GHz Bruker (Rheinstetten, Germany) EMX-EPR spectrometer with a model ER 041 XK-D microwave bridge and equipped with nitrogen gas flow temperature regulation. Samples in 1 mm inner diameter glass capillaries were placed in a standard quartz EPR tube, which contained light silicone oil to maintain thermal stability. Temperature was measured with a fine-wire thermocouple positioned in the silicone oil just above the EPR cavity. The spectrometer settings were as follows: sweep width, 100 G; modulation amplitude, 1.25 G; time constant, 10 ms; modulation frequency, 100 kHz; microwave power, 5 mW.

Simulation of rotationally averaged isotropic spectra was performed with Symphonia (Bruker Spectrospin, Rheinstetten, Germany). These simulated isotropic spectra could be used for spectral subtraction and quantification of the mobile spectral component at high temperatures.

*Thermodynamics of Unfolding*. According to the linear extrapolation model (*24*, *25*), the isothermal free energy of unfolding depends upon denaturant concentration, [urea], according to

$$\Delta G_U = \Delta G_U^{H_2O} - m_G[\text{urea}] \quad (1)$$

where $\Delta G_U^{H_2O}$ is the difference in free energy between the denatured and native states in the absence of denaturant and

$m_G$ is a constant. The free energy of unfolding is obtained from the equilibrium constant, $K_U$, by

$$\Delta G_U = -RT \ln K_U \quad (2)$$

where $T$ is the absolute temperature and $R$ is the ideal gas constant. Assuming a two-state transition (N to U), the equilibrium constant for unfolding is given by

$$K_U = f_U/(1-f_U) \quad (3)$$

where $f_U$ is the fraction of unfolded protein ($f_N + f_U = 1$). From eqs 1−3, the population of unfolded protein is given by

$$f_U = \frac{1}{1+\exp[(\Delta G_U^{H_2O} - m_G[\text{urea}])/RT]} \quad (4)$$

which provides a means of determining the intrinsic free energy of unfolding, $\Delta G_U^{H_2O}$, from the dependence on denaturant concentration.

Generalization to a sequential, multistate equilibrium model for unfolding:

$$N \overset{K_{U,1}}{\longleftrightarrow} I_1 \overset{K_{U,2}}{\longleftrightarrow} I_2 \overset{K_{U,3}}{\longleftrightarrow} \ldots \overset{K_{U,n}}{\longleftrightarrow} I_n \overset{K_{U,n+1}}{\longleftrightarrow} U$$

yields the following expression for the fraction of non-native (total unfolded) protein (*26*):

$$1-f_N = \frac{\sum_{i=1}^{n+1} \exp[-(\Delta G_i^{H_2O} - m_i[\text{urea}])/RT]}{1+\sum_{i=1}^{n+1} \exp[-(\Delta G_i^{H_2O} - m_i[\text{urea}])/RT]} \quad (5)$$

where in terms of the parameters for the individual steps, $j$: $\Delta G_i^{H_2O} = \sum_{j=1}^{i} \Delta G_{U,j}^{H_2O}$ and $m_i = \sum_{j=1}^{i} m_{G,j}$ with a free energy change at each step of $\Delta G_{U,j} = \Delta G_{U,j}^{H_2O} - m_{G,j}[\text{urea}] = -RT \ln(K_{U,j})$.

Relative to a reference temperature $T_o$, the enthalpy and entropy of unfolding at temperature $T$ are given by

$$\Delta H_U^{H_2O}(T) = \Delta H_o + \Delta C_p(T - T_o) \quad (6)$$

and

$$\Delta S_U^{H_2O}(T) = \Delta S_o + \Delta C_p \ln(T/T_o) \quad (7)$$

where $\Delta H_o$ and $\Delta S_o$ are the enthalpy and entropy of unfolding, respectively, at temperature $T_o$ in the absence of denaturant and $\Delta C_p$ is the change in heat capacity on unfolding. If $T_o$ is taken to be the midpoint of the thermal transition in the absence of denaturant, i.e., the temperature ($T_D$) at which the free energy of unfolding is zero ($\Delta G_U^{H_2O} = 0$), then

$$\Delta H_D = T_D \Delta S_D \quad (8)$$

From eqs 6 and 7, the temperature dependence of the free energy of unfolding in water is therefore given by

$$\Delta G_U^{H_2O}(T) = \Delta H_D(1 - T/T_D) + \Delta C_p[T - T_D - T \ln(T/T_D)] \quad (9)$$

where substitution of $\Delta S_D$ has been made from eq 8.

## RESULTS

*EPR Spectra at Different Temperatures*. The EPR spectra of Na,K-ATPase from shark salt gland labeled with 5-MSL on class II −SH groups are shown as a function of temperature in the left-hand panel of Figure 1. Corresponding EPR spectra of Na,K-ATPase from pig kidney, also labeled with 5-MSL according to the class II protocol, are shown in the right-hand panel of Figure 1.

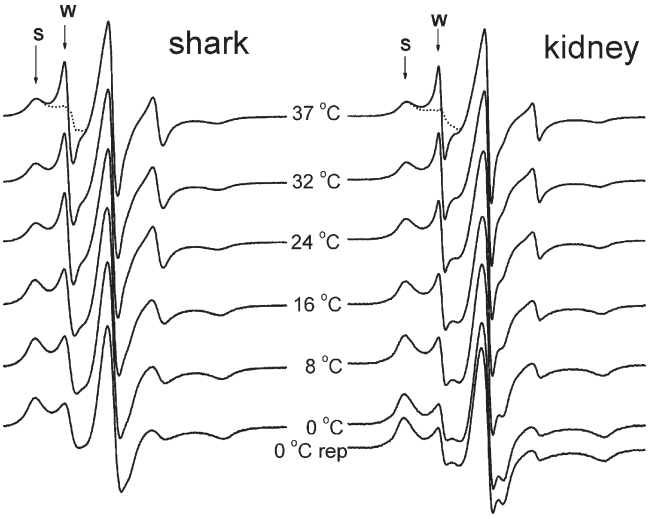


FIGURE 1: Temperature dependence of the EPR spectra from shark (left-hand panel) and kidney (right-hand panel) Na,K-ATPase spin labeled at class II −SH groups with the maleimide nitroxide derivative 5-MSL (pH 7.4). S and W are the $m_I = +1$ manifolds of the strongly and weakly immobilized components, respectively. The dashed lines in the low-field region of the 37 °C spectrum represent the results of subtracting a simulated W-component spectrum that is used to calibrate the normalized line height ratios. 0 °C rep (bottom line) corresponds to the spectrum obtained at 0 °C after the measurement up to 37 °C. Total scan width is 100 G.

The temperature dependences of the EPR spectra of Na,K-ATPase labeled at class II −SH groups indicate an increase in the line height of the weakly immobilized spin-label population (W) with increasing temperature, relative to that of the strongly immobilized component (S), and this effect is completely reversible (see the bottom spectrum on the right in Figure 1). This temperature dependence is due, at least in part, to the differential sensitivity of the two components to rotational motion. The line widths of the weakly immobilized component decrease, whereas those of the strongly immobilized component increase very slightly (accompanied by a small decrease in outer splitting), with increasing temperature. The latter is consistent with an increasing degree of (segmental) motion of the strongly immobilized groups in the slow motion regime of conventional EPR spectroscopy (*27*). Because of the large difference in the spectral range of the two components, the line heights in the first-derivative spectra do not directly reflect the relative proportions of the weakly and strongly immobilized spin labels. Temperature-induced spectral changes of Na,K-ATPase from both sources are completely reversible, also in the presence of urea (data not shown).

*EPR Spectra of Spin-Labeled −SH Groups in the Presence of Urea*. The EPR spectra of 5-MSL-labeled Na,K-ATPase membranes from shark salt gland and from pig kidney in different concentrations of urea (pH 7.4), recorded at 4 °C, are shown in the left-hand and right-hand panels, respectively, of Figure 2. The amplitude of the weakly immobilized component, relative to that of the strongly immobilized component, increases with increasing urea concentration. For all urea concentrations, the EPR spectra (including the relative intensities of the mobile and immobile components) of 5-MSL-labeled Na,K-ATPase from both sources are reversible after urea has been removed from the samples (see the bottom spectra in Figure 2).

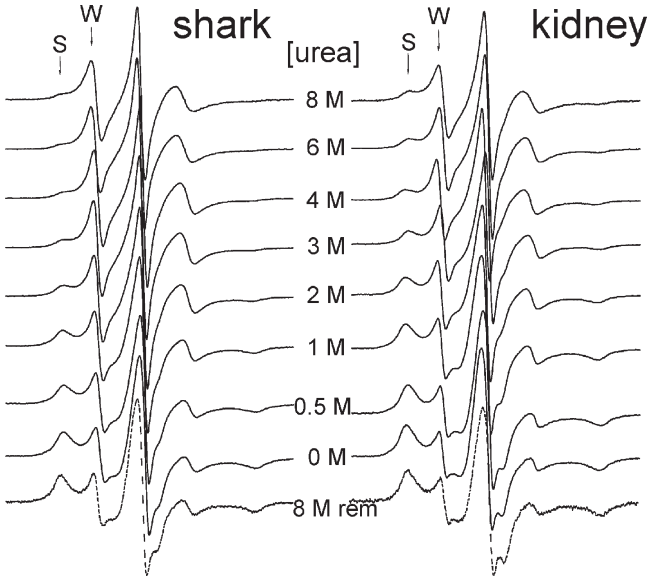


FIGURE 2: EPR spectra of Na,K-ATPase membranes from shark salt gland (left-hand panel) and pig kidney (right-hand panel) spin-labeled at class II −SH groups with 5-MSL. Spectra are shown for samples at 4 °C in increasing concentrations of urea, as indicated. S and W are strongly and weakly immobilized components, respectively. The bottom spectra (8 M rem) are from samples treated with 8 M urea, which was then removed. Total scan width is 100 G.

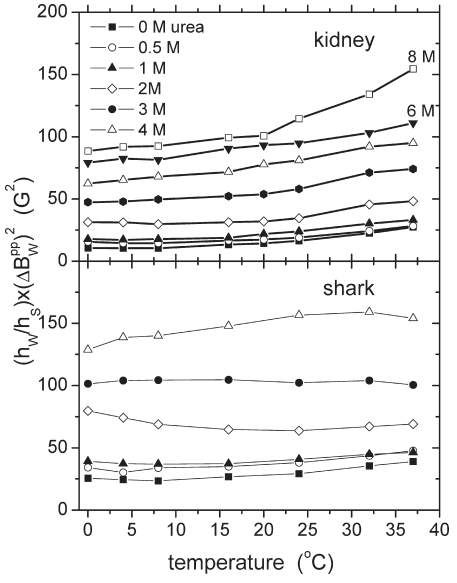


FIGURE 3: Temperature dependence of the line height ratio ($h_W/h_S$) of the low-field resonances from the weakly and strongly immobilized EPR spectral components (W and S, respectively), normalized with the square of the peak-to-peak line width ($\Delta B_W^{pp}$) of the W-line, for spin-labeled Na,K-ATPase in the concentrations of urea indicated. 5-MSL is bound to class II sulfhydryl groups of Na,K-ATPase from pig kidney (top panel) and shark salt gland (bottom panel).

*Urea-Induced Unfolding*. The EPR spectrum is displayed as the first derivative of the absorption spectrum. Double-integrated intensities of the two spectral components are directly proportional to the populations of the two species giving rise to the spectral components. The ratio $h_W \times (\Delta B_W^{pp})^2/h_S$, where $\Delta B_W^{pp}$ is the peak-to-peak line width of the low-field weakly immobilized line, is proportional to the ratio of integrated intensities of the two spectral components, assuming that the width of the strongly immobilized component [i.e., $\Delta B_S^{(1/2)}$] does not vary greatly because this spectrum is in the slow-motion regime.

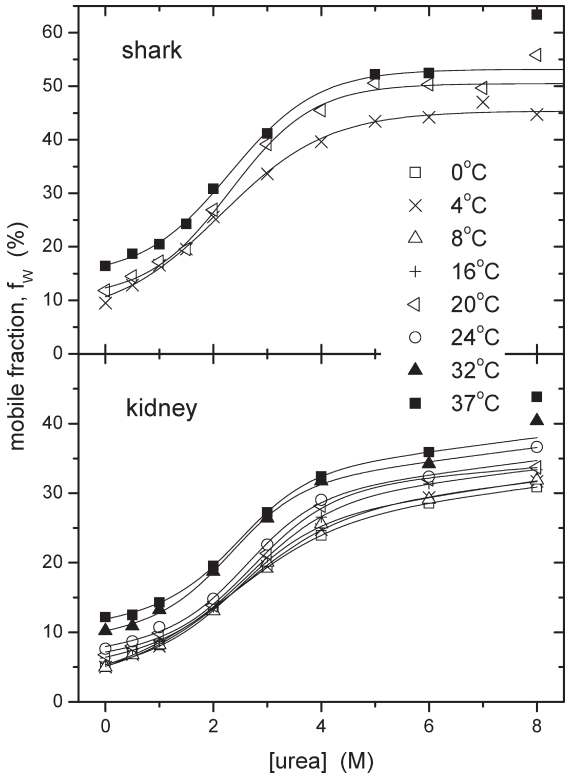


FIGURE 4: Fraction, $f_W$, of the weakly immobilized component in the EPR spectra of shark (top panel) and kidney (bottom panel) Na,K-ATPase labeled with 5-MSL (pH 7.4), as a function of urea concentration, at different temperatures. 5-MSL is covalently bound to class II sulfhydryl groups. Solid lines are least-squares fits of eq 10.

Figure 3 shows the temperature dependence of the ratio of the low-field line heights of the weakly (W) and strongly (S) immobilized components, normalized with the square of the peak-to-peak line width of the W-line, from EPR spectra of urea-treated Na,K-ATPase labeled with 5-MSL. In the absence of urea, the normalized ratio varies relatively little with temperature, indicating that the population of weakly immobilized spin-labels does not increase greatly as the temperature increases.

On the other hand, the normalized line height ratio increases with increasing urea concentration (at constant temperature), indicating that unfolding of the protein in urea leads to an increase in the population of weakly immobilized −SH groups at the expense of the strongly immobilized −SH groups. The normalized line height ratio is also more sensitive to temperature in urea-treated samples. For the kidney enzyme, this sensitivity increases with increasing urea concentrations, as reflected by the slope of the line (Figure 3). The change in normalized line height ratio with increasing urea concentration is reversible after urea has been removed (see Figure 2).

The absolute intensity ratios can be calibrated with spectral subtraction and double integration by using a simulated isotropic spectrum for the weakly immobilized single component at a high temperature [37 °C (see Figure 1)]. This is then used to calibrate the normalized line height ratios in Figure 3, via the 37 °C data. The fractional populations of weakly immobilized −SH groups in the EPR spectra of shark and kidney Na,K-ATPase that are obtained in this way are given as a function of urea concentration, at different temperatures, in Figure 4.

The increase in the population of weakly immobilized spin-labeled −SH groups follows characteristic urea-induced

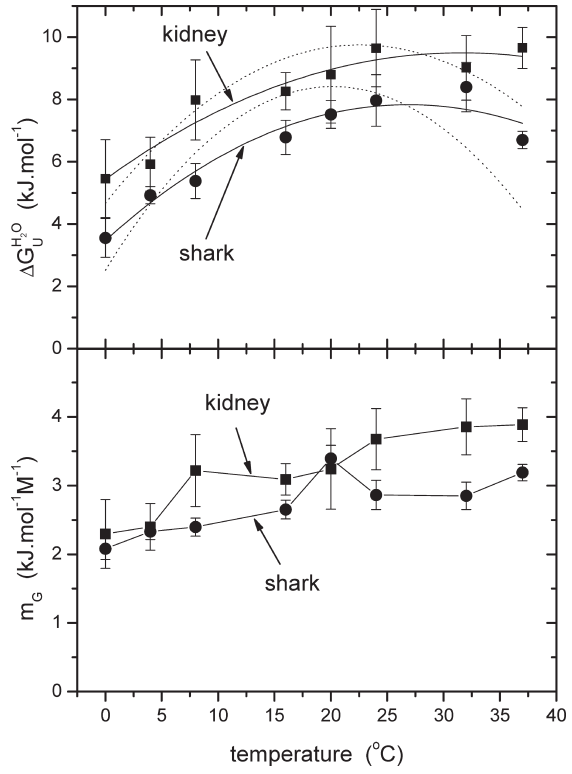


FIGURE 5: Temperature dependence of the free energy of unfolding, $\Delta G_U^{H_2O}$, in water (top panel) and the coefficient, $m_G$, of the dependence on urea concentration (bottom panel) (see eq 1) for shark (●) and kidney (■) Na,K-ATPase from EPR spectra of spin-labeled class II −SH groups. Solid lines in the top panel are least-squares fits of eq 9 (dotted lines are fits with fixed $T_D$ values of 318 and 328 K for shark and kidney, respectively).

unfolding curves (cf. eq 4), which display cooperativity with midpoints in the region of 1.8 and 2−2.5 M urea, for shark and kidney enzymes, respectively. The fraction of weakly immobilized groups increases with increasing temperature in both the folded and unfolded states. In the case of the kidney enzyme, an approximately linear increase in the weakly immobilized population is superimposed upon the unfolding transition. The solid lines in Figure 4 are least-squares fits of the following expression for the fraction, $f_W$, of mobile groups that is based on eq 4 for the fraction of urea-unfolded protein:

$$f_W([\text{urea}]) = \frac{f_W^U - f_W^N}{1+\exp[(\Delta G_U^{H_2O} - m_G[\text{urea}])/RT]} + f_W^N + f_o[\text{urea}] \quad (10)$$

where $f_W^U$ and $f_W^N$ are the fractions of the mobile spectral component in the unfolded (U) and folded (N) states, respectively, assuming a two-state process. The final term, $f_o$[urea], is included to allow for a possible linear baseline increase with increasing urea concentrations that was mentioned in connection with the unfolding curves for the kidney enzyme.

The values of $\Delta G_U^{H_2O}$, the effective free energy of unfolding in water, and $m_G$, the coefficient governing the steepness of urea-induced unfolding, that are obtained from fitting eq 10 to the EPR-detected unfolding curves, assuming a two-state process, are given in Figure 5. The effective free energy of unfolding increases initially with temperature and then reaches a maximum, whereas $m_G$ increases more or less progressively. Fits of the thermodynamic predictions of eq 9 to the temperature dependence of $\Delta G_U^{H_2O}$ are given by the solid lines in Figure 5. Table 1 lists the effective thermodynamic parameters for shark and kidney enzymes that are deduced from these fits.

Table 1: Apparent Thermodynamic Parameters for Na,K-ATPase from Shark Salt Gland and Pig Kidney, Deduced from the Temperature Dependence of Urea-Induced Unfolding Curves According to eqs 1 and 9

| | shark | kidney |
|---|---|---|
| $\Delta G_U^{H_2O}$ at 37 °C (kJ mol$^{-1}$) | 6.7 ± 0.3 | 9.7 ± 0.7 |
| $\Delta H_D$ (kJ mol$^{-1}$) | 139 ± 14 | 130 ± 18 |
| $\Delta C_p$ (kJ mol$^{-1}$ K$^{-1}$) | 3.5 ± 0.7 | 2.4 ± 0.8 |
| $T_D$ (K) | 337 ± 6 (318)[a] | 355 ± 14 (328)[a] |

[a]Heat capacity maximum in differential scanning calorimetry (*17*).

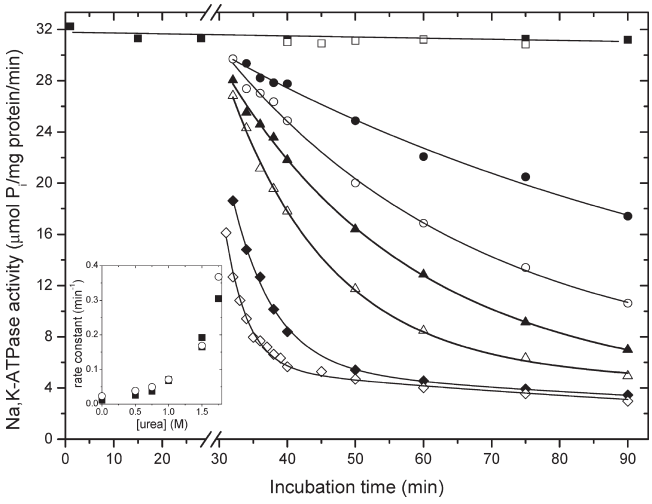


FIGURE 6: Effect of urea on inhibition of shark Na,K-ATPase (0.5 mg/mL) by *N*-ethylmaleimide. Enzyme was incubated with 150 mM KCl, 5 mM CDTA, and 20 mM histidine and with different concentrations of urea at 22 °C. NEM (2 mM) was added to enzyme after incubation for 30 min in the different concentrations of urea. Activity measurements were performed at 37 °C. Controls without NEM in 0 (■) and 0.5 M urea (□). Samples with 2 mM NEM added after preincubation for 30 min with 0 (●), 0.5 (○), 0.75 (▲), 1 (△), 1.5 (◆), and 1.75 (◇) M urea. Specific activity values are given in micromoles of $P_i$ liberated per milligram of protein per minute. The time dependence of inactivation is fitted by a double-exponential function. The inset shows the rate constant for rapid inactivation of Na,K-ATPase activity (■) and K-dependent pNPPase partial reaction (○), as a function of urea concentration.

*Inactivation by Reaction with N-Ethylmaleimide*. To parallel the results obtained with maleimide spin-label reporters attached to class II −SH groups (i.e., those essential to activity), we studied the effects of urea on the rate of inactivation of the Na,K-ATPase by covalent modification of class II groups with NEM. Figure 6 shows the time course of inactivation of the shark enzyme by NEM at 22 °C after preincubation with different concentrations of urea for 30 min. The presence of 0.5 M urea already doubles the inactivation rate, and in 1.5 M urea, inactivation by NEM becomes ~16 times more rapid. The inset of Figure 6 shows the dependence of the rate constant for inactivation by NEM on urea concentration. In the absence of NEM, on the other hand, Na,K-ATPase activity is unaffected by urea over this time period [Figure 6 (□)]. A control experiment showed that removal of urea, after a 30 min incubation, restored the lower NEM sensitivity of the native enzyme (data not shown). Similar results for the urea dependence of the NEM-induced inactivation were also obtained for the $K^+$-dependent *p*-nitrophenylphosphatase partial reaction of the shark enzyme [inset of Figure 6 (○)].

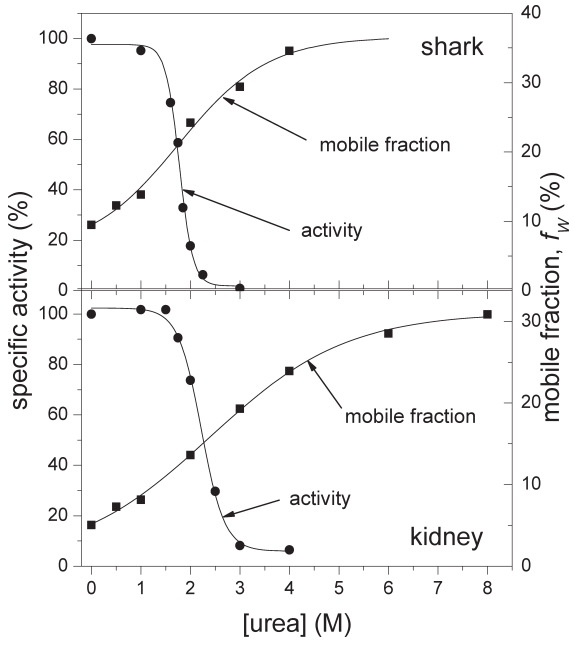


FIGURE 7: Dependence of the specific activity (●) and fraction of mobile spin-labeled −SH groups (■) of shark (top panel) and kidney (bottom panel) Na,K-ATPase on urea concentration. Specific activity corresponds to the ATP hydrolysis activity remaining after incubation of the enzyme in urea for 24 h at 0 °C. Mobile component represents the increase in the weakly immobilized population at 0 °C with increasing urea concentrations, in the EPR spectra of 5-MSL-labeled Na,K-ATPase (pH 7.4) class II −SH groups. Similar buffer conditions were maintained in both experiments.

## DISCUSSION

Most of the class II −SH groups in native Na,K-ATPase (~95%) are immobilized on the nanosecond time scale of conventional EPR, for both shark and kidney enzymes (Figures 1 and 2). The relative proportions of weakly and strongly immobilized components in the EPR spectrum are not responsive to the binding of Na,K-ATPase-specific ligands (*10*). Therefore, the two spectral components most likely correspond to the labeling of different −SH groups. In any case, the weakly immobilized groups constitute a minor population, in the absence of urea.

Treatment with urea converts part of the strongly immobilized class II groups into a weakly immobilized state. For kidney Na,K-ATPase, a small proportion of this population increases linearly with urea concentration. However, for both ATPases, the major increase in mobile population occurs with a dependence on urea concentration that resembles the cooperative unfolding predicted for a two-state model by eq 4. The increase in the population of mobile groups corresponds to those natively immobile groups that are involved in the unfolding process. Depending on temperature, and on the species, the fraction of immobilized class II groups that becomes mobile at high urea concentrations can be up to slightly more than half. This incomplete degree of conversion suggests that only part of the protein is unfolded in high concentrations of urea. It is likely that the transmembrane regions of the protein remain largely unaffected by urea, as is found also to be the case for thermal unfolding of Na,K-ATPase, for which the specific excess heat capacity is considerably lower than that for unfolding of soluble globular proteins (*17*). Also, both the stoichiometry and selectivity of lipid−protein interactions, monitored by the EPR spectra of spin-labeled stearic acid (*28*, *29*), are practically unchanged in 8 M urea (data not shown), therefore evidencing no change in the transmembrane sector. From the protocol and kinetics of labeling, it is possible that up to 50% of the class II groups are localized in the transmembrane sector (*14*). Recent pulsed EPR results on the accessibility of $D_2O$ to spin-labeled class I and class II groups are consistent with this suggestion (*30*).

*Structure−Function Stability Correlation*. Figure 7 compares the EPR-detected urea-induced unfolding curves for shark and pig kidney Na,K-ATPase at 0 °C, with the loss of overall Na,K-ATPase activity upon incubation of the enzyme in urea at 0 °C for 24 h, prior to the standard enzymatic assay. It is seen that Na,K-ATPase from pig kidney is structurally and functionally more stable than Na,K-ATPase from shark salt gland. The denaturant midpoints are 2.25 and ~2.4 M urea for inactivation and unfolding of the kidney enzyme, respectively, and are ~1.8 M urea for both inactivation and unfolding of the shark enzyme. These results on isothermal unfolding are consistent with the difference in thermal stability of Na,K-ATPase from the two sources, as determined by calorimetry (*17*).

The structural and functional stability differences of Na,K-ATPase from shark and kidney could arise from differences in amino acid sequence between the two enzymes. These are located in the extramembranous part of the protein (see the red spheres in Figure 8), which is likely the site of action of urea-induced unfolding. It should be noted that the fraction of weakly immobilized 5-MSL in kidney Na,K-ATPase treated with 6 M urea is larger than that in 3 M urea (Figure 7). This means that the enzyme molecules are not unfolded completely in 3 M urea, although ATP hydrolysis activity is totally lost. Full inactivation occurs before unfolding of the protein is completed.

Three of the amino acids that are not homologous between shark and pig are indicated specifically in Figure 8 (right panel). These are known to have a structural role in Na,K-ATPase function. Arg1005 of kidney (Ser1012 in shark) is involved in regulation by the membrane potential, through alteration of the affinity of the third electrogenic $Na^+$ ion site as part of an arginine cluster (*1*). Ser718 of kidney (Leu725 of shark) participates in coordination of a regulatory cytoplasmic $K^+$ ion (*31*). Glu307 of kidney (Gly314 of shark) is important for the function of the pump under harsh environmental ionic conditions, through regulation of the affinity for external $Na^+$ (*32*). If the stronger effect of urea on stability of the shark enzyme than on that of the kidney enzyme is related to one of these three nonhomologous residues, the stronger candidate would probably be Ser718, which is positioned well away from the bilayer core (the two other residues are close to the bilayer and associated with α-helical structures that might be more resistant to urea). Further, the extent of homology between the $\beta$-subunits (81%) and between the $\gamma$-subunits (57%) of shark and pig Na,K-ATPases is less than that between the α-subunits (94%). This could also be a contributory factor to the species difference, if the smaller subunits are important for enzyme stability.

For both enzymes, the unfolding monitored by the increase in the population of weakly immobilized −SH groups, although having a similar midpoint, takes place over a broader range of urea concentrations than does the loss of enzyme activity, even after subtraction of a linearly sloping baseline (see Figure 7). To explore potential functional effects of unfolding at urea concentrations lower than that which has any effect on the overall Na,K-ATPase activity, we checked the effects of urea on the rate of inactivation of the enzyme activity by NEM (see Figure 6). Very low concentrations of urea produce reversible unfolding of Na,K-ATPase; this reversible unfolding does not affect overall

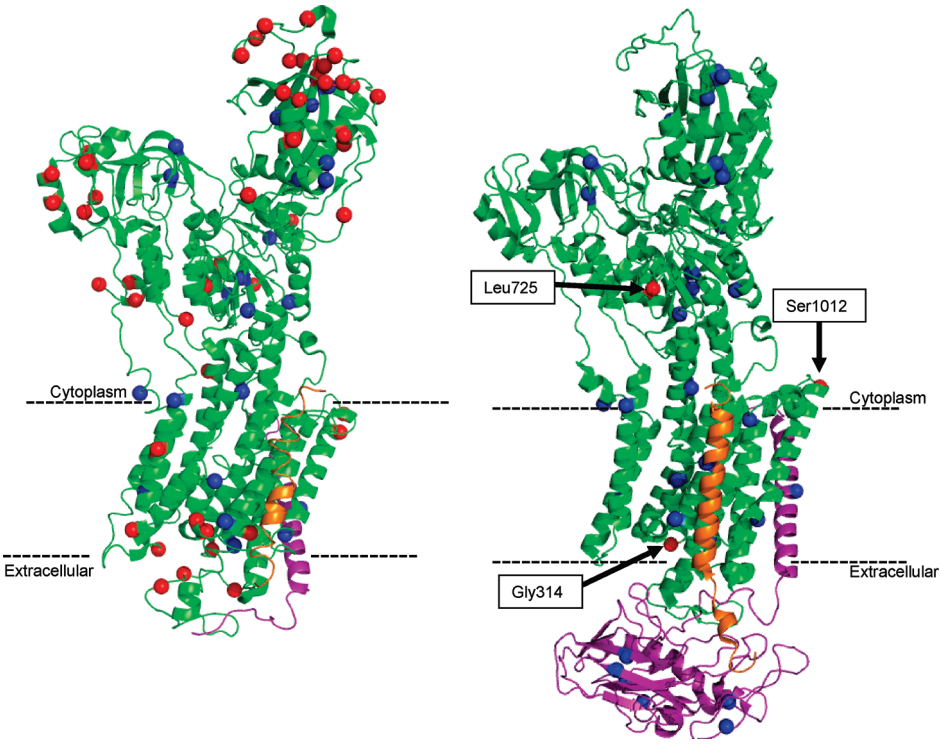


FIGURE 8: Crystal structures of Na,K-ATPase from (left) pig kidney (*1*) (PDB entry 3b8e) and (right) shark salt gland (*2*) (PDB entry 2zxe). The α-subunit is shown in green, and the *β*- and *γ*-subunits in purple and orange, respectively. Cysteine residues are depicted as blue spheres, and amino acids not homologous between pig and shark enzymes are highlighted as red spheres in the left panel. The number and positions of the cysteine residues in the α-subunit are identical for shark and kidney Na,K-ATPases. Only one nonhomologous amino acid (Ala131 in kidney and Thr138 in shark) is located in the transmembrane region. In the right panel, three nonhomologous amino acids (red spheres) marked with arrows (Gly314, Leu725, and Ser1012 in shark; Glu307, Ser718, and Arg1005 in kidney) are known to have clear functional roles (see the text).

ATPase activity (see Figure 7). However, this partial unfolding facilitates the reaction of NEM with class II −SH groups, which leads to rapid enzyme inactivation.

*Thermodynamics of Unfolding*. The EPR detection of urea-induced unfolding allows estimation of effective thermodynamic parameters governing the overall unfolding process. The values given in Table 1 can be compared with calorimetric measurements of thermal unfolding of the two Na,K-ATPases (*17*). The value of $T_D$ deduced for the kidney enzyme is greater than that for shark, in line with the relative positions of the heat capacity maxima for thermal unfolding of the two proteins. However, the absolute values of $T_D$ obtained from fitting the temperature dependences of the denaturant-induced unfolding are greater than the midpoint temperatures for thermal denaturation in the absence of urea. The dotted lines in Figure 5 show the results of fitting eq 9 with $T_D$ fixed equal to the temperature of the calorimetric maximum in excess heat capacity. Also, the effective unfolding enthalpy ($\Delta H_D$) is much lower than that of even a single component in the multicomponent denaturation endotherms. These latter range from 335 to 580 kJ mol$^{-1}$ for the shark enzyme and from 410 to 815 kJ mol$^{-1}$ for the enzyme from pig kidney (*17*). Additionally, it is evident from Figure 7 (cf. eq 4) that the effective free energy of unfolding that is deduced from activity measurements ($\Delta G_U^{H_2O}$ = 21.5 ± 2.3 kJ mol$^{-1}$ and $m_G$ = 9.7 ± 1.0 kJ mol$^{-1}$ M$^{-1}$ for kidney) is much greater than that associated with the transition to a mobile population of −SH groups ($\Delta G_U^{H_2O}$ = 5.5 ± 1.3 kJ mol$^{-1}$ and $m_G$ = 2.3 ± 0.5 kJ mol$^{-1}$ M$^{-1}$ for kidney). This difference is also observed for the shark enzyme, for which the effective free energy of unfolding deduced from activity measurements ($\Delta G_U^{H_2O}$ = 28.8 ± 6.0 kJ mol$^{-1}$ and $m_G$ = 16.2 ± 3.4 kJ mol$^{-1}$ M$^{-1}$ for shark) also is much greater than that associated with the transition to a mobile population of −SH groups ($\Delta G_U^{H_2O}$ = 3.55 ± 0.6 kJ mol$^{-1}$ and $m_G$ = 2.1 ± 0.15 kJ mol$^{-1}$ M$^{-1}$ for shark).

Quite possibly, thermal denaturation gives rise to a greater degree of unfolding than that which results from the limited accessibility of urea to the membranous enzyme. Another possible reason for the apparent difference between thermal and urea-induced unfolding is that conversion from immobile to mobile −SH groups may involve "softer" interactions than those governing the transition to an unfolded or denatured state, although they must be strongly influenced by the latter. Hence, limited conversion to mobile groups may precede global unfolding and possibly may even continue further beyond this event. In this connection, it is interesting to note that site-directed spin labeling of the FepA protein has revealed different denaturant unfolding sensitivities depending on the local environment (*33*).

A further reason for differences in the effective values deduced for the thermodynamic parameters is seen in Figure 6. Conformational changes that increase the accessibility of NEM to those −SH groups, which are essential for enzyme activity, precede the unfolding event that abolishes overall Na,K-ATPase activity. Whereas the dependence of the population of mobile groups on denaturant concentration can be modeled adequately by a two-state transition (eq 10), this does not exclude the possibility that other transitions take place but are unresolved from the main unfolding transition. The inactivation data, which are given in the inset of Figure 6, suggest one possible such

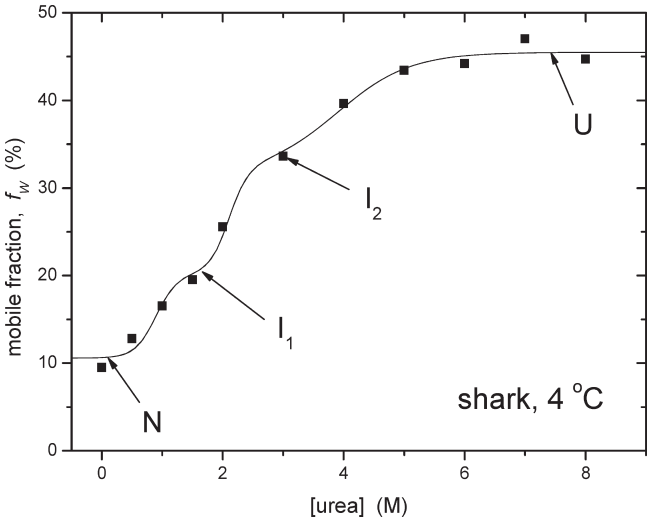


FIGURE 9: Simulation of four-state unfolding ($N \xleftrightarrow{K_{U,1}} I_1 \xleftrightarrow{K_{U,2}} I_2 \xleftrightarrow{K_{U,3}} U$) of shark Na,K-ATPase at 4 °C (■, experimental data), as a function of urea concentration. The solid line is a calculation according to eq 11 for two intermediates, with the following parameters: $\Delta G^{H_2O}_{U,1} = 11.9$ kJ mol$^{-1}$, $m_{G,1} = 5.75$ kJ mol$^{-1}$ M$^{-1}$; $\Delta G^{H_2O}_{U,2} = 29.7$ kJ mol$^{-1}$, $m_{G,2} = 6.15$ kJ mol$^{-1}$ M$^{-1}$; and $\Delta G^{H_2O}_{U,3} = 15.0$ kJ mol$^{-1}$, $m_{G,3} = 1.67$ kJ mol$^{-1}$ M$^{-1}$.

pretransition occurring at lower urea concentrations and/or with lower cooperativity, $m_G$.

*Multistate Unfolding*. For unfolding that involves more than one step, generalization of eq 10 (on the basis of eq 5) gives the following expression for the total fraction of mobile spin-labeled −SH groups:

$$f_W([\text{urea}]) = \frac{\sum_{i=1}^{n+1} (f_W^{I_i} - f_W^{I_{i-1}}) \exp[-(\Delta G_i^{H_2O} - m_i[\text{urea}])/RT]}{1 + \sum_{i=1}^{n+1} \exp[-(\Delta G_i^{H_2O} - m_i[\text{urea}])/RT]} + f_W^N \quad (11)$$

where $f_W^{I_i}$ is the fraction of mobile spectral component in state $I_i$. With this nomenclature, $I_0$ is the native state (N), in the absence of urea, and $I_{n+1}$ is the final unfolded state (U). Figure  gives the predictions of eq 11 for four-state unfolding (i.e., $n = 2$ intermediates), compared with the experimental results for shark Na,K-ATPase at 4 °C. For this simulation, the parameters $\Delta G^{H_2O}_{U,1}$ and $m_{G,1}$ that govern the first step are fixed at values that give unfolding at low urea concentrations where inactivation by NEM is already found (inset of Figure 6). Similarly, $\Delta G^{H_2O}_{U,2}$ and $m_{G,2}$ are fixed at values close to those characterizing inactivation of the overall Na,K-ATPase reaction (top panel of Figure 7). Under these constraints, two steps are insufficient to describe the whole of the unfolding detected by the increase in population of mobile spin labels. A third unfolding step, i.e., a second intermediate, is the minimum that is required to simulate the complete unfolding curve. An adequate description of the data can be achieved with this four-state model $N \xleftrightarrow{K_{U,1}} I_1 \xleftrightarrow{K_{U,2}} I_2 \xleftrightarrow{K_{U,3}} U$ but the pronounced structure evident in the simulation will be smoothed out by inclusion of further intermediate steps. This would result in a broad sigmoidal envelope that is well fit by a two-state model with lower cooperativity, as is found experimentally. Most probably, an extended hierarchy of structural transitions is involved in the unfolding of a protein with the degree of complexity of the Na,K-ATPase.

The simulation in Figure  is able, therefore, to reconcile the different sensitivities to unfolding that are registered by the various functional and structural indicators. This strongly suggests that a multistep unfolding takes place via several intermediates, not all of which are necessarily as distinct as those recorded by the functional activities or the minimal three-step model of Figure .

## CONCLUSION

Urea-induced structural changes lead to the inhibition of Na,K-ATPase activity. Structural changes detected by EPR spectroscopy are reversible over the whole range of urea concentrations (0−8 M), although activity loss is always irreversible. The structure at the cytoplasmic side is more flexible and fragile relative to the transmembrane part of the Na,K-ATPase and thus is more sensitive to the effect of denaturant. Conformational changes at the active thiol groups of these enzymes indeed take place before unfolding of the enzymes as a whole together with enzyme inactivation. Na,K-ATPase from pig kidney is not only more stable to thermal denaturation but also more stable to urea-induced denaturation, relative to the Na,K-ATPase from shark salt gland.

## REFERENCES

1. Morth, J. P., Pedersen, B. P., Toustrup-Jensen, M. S., Sørensen, T. L.-M., Petersen, J., Andersen, J. P., Vilsen, B., and Nissen, P. (2007) Crystal structure of the sodium-potassium pump. *Nature 450*, 1043–1050.
2. Shinoda, T., Ogawa, H., Cornelius, F., and Toyoshima, C. (2009) Crystal structure of the sodium-potassium pump at 2.4 Å resolution. *Nature 459*, 446–450.
3. Kaplan, J. H., and De Weer, P. (1991) The Sodium Pump: Structure, Mechanism and Regulation , Rockefeller University Press, New York.
4. Skou, J. C. (1990) The energy coupled exchange of $Na^+$ for $K^+$ across the cell membrane: The $Na^+$,$K^+$-pump. *FEBS Lett. 268*, 314–324.
5. Schoot, B. M., Schoots, A. F. M., de Pont, J. J. H. H. M., Schuurmans-Stekhoven, F. M. A. H., and Bonting, S. L. (1977) Studies on ($Na^+$+$K^+$) activated ATPase. 41. Effects of *N*-ethylmaleimide on overall and partial reactions. *Biochim. Biophys. Acta 483*, 181–192.
6. Winslow, J. W. (1981) The reaction of sulfhydryl groups of sodium and potassium-activated adenosine triphosphatase with *N*-ethylmaleimide: The relationship between ligand-dependent alterations of nucleophilicity and enzymatic conformational states. *J. Biol. Chem. 256*, 9522–9531.
7. Kirley, T. L., Lane, L. K., and Wallick, E. T. (1986) Identification of an essential sulfhydryl group in the ouabain binding site of (Na,K)-ATPase. *J. Biol. Chem. 261*, 4525–4528.
8. Patzelt-Wenczler, R., Pauls, H., Erdmann, E., and Schoner, W. (1975) Evidences for a sulfhydryl group in ATP-binding site of ($Na^+$+$K^+$)-activated ATPase. *Eur. J. Biochem. 53*, 301–311.
9. Esmann, M. (1982) Sulfhydryl groups of ($Na^+$+$K^+$)-ATPase from rectal glands of *Squalus acanthias*: Titration and classification. *Biochim. Biophys. Acta 688*, 251–259.
10. Esmann, M. (1982) Sulfhydryl groups of ($Na^+$+$K^+$)-ATPase from rectal glands of *Squalus acanthias*: Detection of ligand induced conformational changes. *Biochim. Biophys. Acta 688*, 260–270.
11. Wallick, E. T., Anner, B. M., Ray, M. V., and Schwartz, A. (1978) Effect of temperature on phosphorylation and ouabain binding to *N*-ethylmaleimide-treated ($Na^+$,$K^+$)-ATPase. *J. Biol. Chem. 253*, 8778–8786.
12. Esmann, M., and Klodos, I. (1983) Sulphydryl groups of the Na,K-ATPase: Effects of *N*-ethyl-maleimide on phosphorylation from ATP in the presence of $Na^+$ + $Mg^{++}$. In Structure, Mechanism and Function of the Na/K-Pump (Hoffman, J. F., and Forbush, B., III, Eds.) pp 349−352, Academic Press, New York.
13. Ning, G., Maunsbach, A., and Esmann, M. (1993) Ultrastructure of membrane-bound Na,K-ATPase after extensive tryptic digestion. *FEBS Lett. 330*, 19–22.
14. Esmann, M., Karlish, S. J. D., Sottrup-Jensen, L., and Marsh, D. (1994) Structural integrity of the membrane domains in extensively trypsinized Na,K-ATPase from shark rectal glands. *Biochemistry 33*, 8044–8050.

15. Esmann, M., Horváth, L. I., and Marsh, D. (1987) Saturation-transfer electron spin resonance studies on the mobility of spin-labeled sodium and potassium ion activated adenosinetriphosphatase in membranes from *Squalus acanthias*. *Biochemistry 26*, 8675–8683.
16. Esmann, M., Hankovszky, H. O., Hideg, K., and Marsh, D. (1989) A novel spin-label for study of membrane protein rotational diffusion using saturation transfer electron spin resonance. Application to selectively labelled class I and class II -SH groups of the shark rectal gland $Na^+/K^+$-ATPase. *Biochim. Biophys. Acta 978*, 209–215.
17. Fodor, E., Fedosova, N. U., Ferencz, C., Marsh, D., Páli, T., and Esmann, M. (2008) Stabilization of Na,K-ATPase by ionic interactions. *Biochim. Biophys. Acta 1778*, 835–843.
18. Jorge-García, I., Bigelow, D. J., Inesi, G., and Wade, J. B. (1988) Effect of urea on the partial reactions and crystallization pattern of sarcoplasmic reticulum adenosine triphosphatase. *Arch. Biochem. Biophys. 265*, 82–90.
19. Skou, J. C., and Esmann, M. (1979) Preparation of membrane-bound and of solubilized ($Na^+$+$K^+$)-ATPase from rectal glands of *Squalus acanthias*. The effect of preparative procedures on purity, specific and molar activity. *Biochim. Biophys. Acta 567*, 436–444.
20. Jørgensen, P. L. (1974) Purification and characterization of ($Na^+$+$K^+$)-ATPase. III. Purification from the outer medulla of mammalian kidney after selective removal of membrane components by sodium dodecyl sulphate. *Biochim. Biophys. Acta 356*, 36–52.
21. Klodos, I., Esmann, M., and Post, R. L. (2002) Large-scale preparation of sodium-potassium ATPase from kidney outer medulla. *Kidney Int. 62*, 2097–2100.
22. Fiske, C. H., and Subbarow, Y. (1925) The colorimetric determination of phosphorus. *J. Biol. Chem. 66*, 375–400.
23. Esmann, M. (1988) ATPase and phosphatase activity of the $Na^+$,$K^+$-ATPase: Molar and specific activity, protein determinations. *Methods Enzymol. 156*, 105–115.
24. Schellmann, J. A. (1978) Solvent denaturation. *Biopolymers 17*, 1305–1322.
25. Makhatadze, G. I. (1999) Thermodynamics of protein interactions with urea and guanidinium hydrochloride. *J. Phys. Chem. B 103*, 4781–4785.
26. Patel, S., Chaffotte, A. F., Goubard, F., and Pauthe, E. (2004) Urea-induced sequential unfolding of fibronectin: A fluorescence spectroscopy and circular dichroism study. *Biochemistry 43*, 1724–1735.
27. Esmann, M., Hideg, K., and Marsh, D. (1992) Conventional and saturation transfer EPR spectroscopy of Na,K-ATPase modified with different maleimide-nitroxide derivatives. *Biochim. Biophys. Acta 1159*, 51–59.
28. Esmann, M., and Marsh, D. (1985) Spin-label studies on the origin of the specificity of lipid-protein interactions in $Na^+$,$K^+$-ATPase membranes from *Squalus acanthias*. *Biochemistry 24*, 3572–3578.
29. Esmann, M., and Marsh, D. (2006) Lipid-protein interactions with the Na,K-ATPase. *Chem. Phys. Lipids 141*, 94–104.
30. Guzzi, R., Bartucci, R., Sportelli, L., Esmann, M., and Marsh, D. (2009) Conformational heterogeneity and spin-labelled -SH groups: Pulsed EPR of Na,K-ATPase. *Biochemistry 48*, 8343–8354.
31. Schack, V. R., Morth, J. P., Toustrup-Jensen, M. S., Anthonisen, A. N., Nissen, P., Andersen, J. P., and Vilsen, B. (2008) Identification and function of a cytoplasmic $K^+$ site of the $Na^+$,$K^+$-ATPase. *J. Biol. Chem. 283*, 27982–27990.
32. Colina, C., Rosenthal, J. J. C., De Giorgis, J. A., Srikumar, D., Iruku, N., and Holmgren, N. (2007) Structural basis of $Na^+/K^+$-ATPase adaptation to marine environments. *Nat. Struct. Mol. Biol. 14*, 427–431.
33. Klug, C. S., and Feix, J. B. (1998) Guanidine hydrochloride unfolding of a transmembrane $\beta$-strand in FepA using site-directed spin labeling. *Protein Sci. 7*, 1469–1476.